Invited Paper

Ultrasonic Sensing and Time-Frequency Analysis for Detecting Plastic Deformation in an Aluminum Plate

Lindsey Channels[a], Debejyo Chakraborty[b], Donna Simon[b], Narayan Kovvali*[b], James Spicer[a], Antonia Papandreou-Suppappola[b], Douglas Cochran[b], Pedro Peralta[c], and Aditi Chattopadhyay[c]

[a]Department of Materials Science and Engineering, Johns Hopkins University, Baltimore, MD
[b]Department of Electrical Engineering, Arizona State University, Tempe, AZ
[c]Department of Mechanical and Aerospace Engineering, Arizona State University, Tempe, AZ

ABSTRACT

We investigate the use of low frequency (10-70 MHz) laser ultrasound for the detection of fatigue damage. While high frequency ultrasonics have been utilized in earlier work, unlike contacting transducers, laser-based techniques allow for simultaneous interrogation of the longitudinal and shear moduli of the fatigued material. The differential attenuation changes with the degree of damage, indicating the presence of plasticity. In this paper, we describe a structural damage identification approach based on ultrasonic sensing and time-frequency techniques. A parsimonious representation is first constructed for the ultrasonic signals using the modified matching pursuit decomposition (MMPD) method. This decomposition is then employed to compute projections onto the various damage classes, and classification is performed based on the magnitude of these projections. Results are presented for the detection of fatigue damage in Al-6061 and Al-2024 plates tested under 3-point bending.

Keywords: structural health monitoring, ultrasonic sensing, damage detection, time-frequency analysis, matching pursuit decomposition

1. INTRODUCTION

Sensing technologies have always played a central role in the design and deployment of structural health monitoring (SHM) systems.[1–3] Traditional contact transducers are used to generate and detect acoustic waves in materials but have limiting factors. They require correct coupling to a material as well as a surface area that can accommodate the transducer.[4] The use of laser-generated high-frequency ultrasound on a metal surface began in the 1960s for the characterization of bulk and surface material properties.[4,5] Generation of this ultrasound can be made with high or low power depending on how much energy is desired from the laser pulse. At a very high power, ablation of the specimen will result, and at a low power, non destructive thermoelastic generation of ultrasound occurs.[5] In non-ablation ultrasonics, a short-pulse laser irradiates the sample causing localized heating and in turn thermal expansion which induces a strain field. The energy from the strain field produces elastic or ultrasonic waves. This is a thermoelastic process that happens at low energies and leaves the specimen unharmed.[4,6] To implement an entirely laser-based system, a Michelson-type interferometer is positioned opposite the source and is used as a detector with that side of the sample acting as a reflecting surface.[4] Advantages of using a laser based ultrasonic generation and detection system over piezoelectric transducers include but are not limited to: entirely non-contact, remote actuation, useful for specimens with complicated geometries, point source capability, broadband frequencies, reproducible measurements, generation of bulk and surface waves, and high spatial resolution with the short times involved making the measurements local.[4–6]

Characterization of materials and structures using laser pulses within the thermoelastic regime has been heavily investigated. Scruby et al. used a Q-switched Nd:YAG laser and recorded the acoustic waveforms under different conditions, but still implemented a capacitance transducer over an interferometer to receive these generated waves.[7] Blodgett and Baldwin have used laser ultrasonics to determine the effects of bulk treatments on the high-temperature elastic moduli of sapphire for IR transparent windows in endo-atmospheric missiles.

*Narayan.Kovvali@asu.edu; phone 1 480 965 5954

Modeling, Signal Processing, and Control for Smart Structures 2008, edited by Douglas K. Lindner
Proc. of SPIE Vol. 6926, 69260P, (2008) · 0277-786X/08/$18 · doi: 10.1117/12.776625

Measurements were originally performed using contact transducers, but the couplant and the transducer limited the maximum temperature. Blodgett and Baldwin applied the non-contact laser method to inspect the sapphire samples at temperatures approaching 1700 °C. They also cited the use of laser-based ultrasound for inspection of the bonding agent between a glass cover slip and the thin solar panel structures on spacecraft, and for assessing tooth health to identify decay in its earliest stages before x-ray detection.[4]

Operating the laser in the ablative regime has also proved to be useful when generating ultrasound at high temperatures and long path lengths in order to achieve a high signal to noise ratio. Mi and Ume used a laser-based system and investigated the frequency spectra of ultrasound in the ablative regime. They determined that the type of material, thickness of the material, and laser power density affected the center frequency and frequency distribution of the generated ultrasound.[6]

The detection of surface cracks has been explored using laser generated surface waves with the generator and the detector on the same side of the sample.[5,8] Arias and Achenbach have developed a model for the scanning laser source (SLS) technique for the detection of surface breaking cracks. Their inspection method shows that a surface breaking crack smaller than the wavelength of the Rayleigh wave generated on the surface can be detected.[5] Other types of ultrasonic generation and detection use electromagnetic acoustic resonance (EMAR) to measure attenuation and resonant frequency along with a non-contacting electromagnetic acoustic transducer (EMAT). Ogi et al. use this method to sense fatigue damage in rotating bending test of steel pipes and detect the anomalies that indicate crack initiation in a location before that crack formation is visible with current inspection techniques. Their results show an elevated attenuation peak at 80%-90% of the fracture life. The data collected yields the ability to calculate dislocation density and dislocation loop length.[9]

In this work, a non-contact ultrasonic technique using laser generation and detection has been implemented. This technique was chosen since it allows for a broadband (1-60 MHz) signal acquisition capable of gathering information about the longitudinal and shear wave stiffnesses in a single measurement. Instead of using a contact transducer with a large aperture size, the 0.1 mm laser spot size used here allows for relatively high spatial resolution measurements. Data can be matched approximately to a model developed by Rose[10] to investigate the changes in wavespeed and attenuation that are potentially due to interactions with the mesoscopic changes in the material structure as damage accumulates.

The detection and classification of damage is carried out here using time-frequency analysis.[11] Specifically, we employ the time-frequency technique of matching pursuit decomposition (MPD)[12] to construct a parsimonious representation for the ultrasonic signals. The representation decomposes the given signals into weighted linear combinations of basis functions selected from a pre-defined dictionary. The dictionary can be adapted[13] to suit the time-spectral characteristics of the signals of interest. Our work relies on using a dictionary composed of real measured data, and the resulting algorithm known as the modified matching pursuit decomposition (MMPD)[14,15] can be utilized very effectively for the task of classification.[14–20] The classifier makes use of the MMPD to compute projections onto the various damage classes and classifies signals based on the magnitude of these projections. We apply the MMPD classifier for the detection of fatigue damage in Al-6061 and Al-2024 plates tested under 3-point bending and present classification results showing its performance on the ultrasonic data.

The remainder of this paper is organized as follows. Section 2 describes the time-frequency based classification algorithm. Section 3 presents an application of the ultrasonic sensing and the damage classifier to the detection of fatigue damage in aluminum plates.

2. TIME-FREQUENCY BASED CLASSIFIER

In this section we briefly review the analytical framework used in the proposed damage classification algorithm. For more details on these topics, the reader is referred to the literature.[12–17]

2.1 Matching Pursuit Decomposition

The matching pursuit decomposition (MPD)[12] is a representation for signals in terms of basis functions chosen from a redundant dictionary. A given signal $s(t) \in \mathbf{L}^2(\mathbb{R})$ is iteratively decomposed into the linear expansion

$$s(t) = \sum_{l=0}^{L-1} \alpha_l \, g_{\gamma_l}(t) + R_L s(t), \tag{1}$$

where $R_L s(t)$ denotes the residue after the L MPD iterations (with $R_0 s(t) \equiv s(t)$). The expansion coefficients α_l, given by

$$\alpha_l = \int_{-\infty}^{\infty} R_l s(t) \, g_{\gamma_l}^*(t) \, dt, \;\; l = 0, \ldots, L-1, \tag{2}$$

are the inner-products between the residues $R_l s(t)$ and the basis functions $g_{\gamma_l}(t) \in \mathbf{L}^2(\mathbb{R})$ which are selected from a dictionary $\mathcal{D} = \{g_\gamma(t)\}_{\gamma \in \Gamma}$ so as to maximize the magnitude of the inner-products in (2) at each step of the iteration:

$$g_{\gamma_l}(t) = \underset{g_\gamma \in \mathcal{D}}{\operatorname{argmax}} \left| \int_{-\infty}^{\infty} R_l s(t) \, g_\gamma^*(t) \, dt \right|. \tag{3}$$

The basis functions (atoms) in the expansion are therefore selected in order to best match the signal structure, resulting in an adaptive signal representation.

At each iteration, the residue decreases in energy: $\|R_{l+1} s(t)\|^2 \leq \|R_l s(t)\|^2$ (here $\|\cdot\|$ is the 2-norm), and convergence holds in the $\mathbf{L}^2$ sense:[12]

$$\lim_{L \to \infty} \|s(t) - \sum_{l=0}^{L-1} \alpha_l \, g_{\gamma_l}(t)\|^2 = \lim_{L \to \infty} \|R_L s(t)\|^2 = 0. \tag{4}$$

After L iterations, the MPD results in the unique approximation (truncated MPD representation)

$$s_L(t) = \sum_{l=0}^{L-1} \alpha_l \, g_{\gamma_l}(t) \approx s(t) \tag{5}$$

in terms of the selected family of basis functions.

In applications, the truncation limit L is usually chosen such that the energy of the residue after L iterations is smaller than some pre-defined value. This is to ensure that the MPD extracts the most important signal components of interest, while effectively filtering out unwanted components such as noise.

The dictionary $\mathcal{D}$ employed in the MPD need not be orthonormal but is required to be complete.[12] Time-frequency-scale dictionaries based on Gaussian atoms[12] have been quite popular because they yield adaptive time-frequency representations. In the modified matching pursuit decomposition (MMPD) algorithm,[13,17] the dictionary is composed of time-frequency shifted and scaled signals of real sensor data (here obtained from structural damage experiments). Specifically, the $g_{\gamma_l}(t)$ in (1) is given by

$$g_{\gamma_l}(t) = \frac{C}{\sqrt{s_l}} \, g\left(\frac{t - \tau_l}{s_l} \right) \cos(2\pi \nu_l t), \tag{6}$$

where the basic atoms $g(t)$ are the measured signals that are chosen to represent all possible signals in the application, $\gamma_l = (s_l, \tau_l, \nu_l)$ denotes the set of scale, time-shift, and frequency-shift parameters applied to the basic atom, and C is a normalizing constant such that $\|g_{\gamma_l}(t)\| = 1$. Since this dictionary is matched specifically to the signals of interest in the application, it has the advantage of yielding highly parsimonious representations.

2.2 Modified Matching Pursuit Decomposition based Classifier

We now describe the MMPD based classification scheme.[14–16] The approach relies on the fact that the class membership information is available for the "training" signals which are used to build the MMPD dictionary. Specifically, the MMPD is performed as described in the previous subsection with the dictionary atoms $g_{\gamma_l}(t)$ of (1) now being real measured training signals from all the (say, M) classes, each of which is time-frequency shifted and scaled to cover the entire time-frequency plane.

Consider the MMPD of a test signal $s^{\text{test}}(t)$, given by

$$s^{\text{test}}(t) = \sum_{l=0}^{L-1} \alpha_l \, g_{\gamma_l}(t) + R_L s(t). \tag{7}$$

We define indicator variables $\{m_l\}_{l=0,\ldots,L-1}$ which indicate the class to which the lth atom $g_{\gamma_l}(t)$ in the decomposition (7) belongs, for $l = 0, \ldots, L-1$. So $m_l = k$, if $g_{\gamma_l}(t)$ is a time-frequency shifted and scaled signal from class k (with $k \in \{1, \ldots, M\}$). We can then construct the sum

$$\rho_k = \sum_{l=0}^{L-1} |\alpha_l|^2 \, \delta_{m_l,k}, \tag{8}$$

which is the projection of the test signal $s^{\text{test}}(t)$ on to the subspace spanned by atoms from class k (here δ denotes the Kronecker delta symbol). The residue R_L is assumed to be small enough to be ignored, which is frequently the case even for moderate values of L owing to the sparsity of the representation. To see this, note that the delta function restricts the sum to only those values of l for which $m_l = k$ (in other words, to only those atoms which belong to class k).

The quantity ρ_k essentially measures the magnitude of the signal's projection on to class k, and the test signal $s^{\text{test}}(t)$ is classified to that class k^* which maximizes this projection:

$$k^* = \underset{k=1,\ldots,M}{\text{argmax}} \, \rho_k. \tag{9}$$

The algorithm requires the computation of the projections ρ_k for $k = 1, \ldots, M$ in (8), which in turn requires keeping track of the class membership variables $\{m_l\}_{l=0,\ldots,L-1}$.

3. APPLICATION TO THE DETECTION OF FATIGUE DAMAGE IN ALUMINUM PLATES

In this section, we describe an application of the laser ultrasonic sensing and the time-frequency based classification technique for the detection of fatigue damage in aluminum plates tested under 3-point bending.

3.1 Experimental setup and data collection

The samples used for these experiments are aluminum 6061-T6 plates, with a mirror finish and cut into 3.5" x 0.7" x 0.125" bars. Aluminum 2024-T351 plates (Figure 1(a)) were also used, which were cut into the same bar size and polished to a mirror finish on one side. The mirror finish is necessary for the interferometric detection and also eliminates surface defects that have the potential to be locations for crack initiation during the cyclic loading. The samples were fatigued on a three-point bend fixture (see Figure 1(b)), with a 75 lb load at 5 Hz. This results in a maximum bending stress of approximately 245 MPa, which is about 75% of the yield stress. Every 10,000 cycles, the fatigue process was interrupted and samples were evaluated with the laser-ultrasonic system in order to monitor any changes that might occur within the specimen's lifetime. The damage itself is at or below the grain level (about 100 μm), and is not visible to naked eye for low fatigue levels such as 40,000 cycles. For higher fatigue levels like 70,000-100,000 cycles, surface damage was visible in the form of fatigue-induced surface roughness.

The sensing experimental apparatus (Figure 2) consists of a pulsed Nd:YAG laser ($\sim$10 ns pulse FWHM, 1064 nm) with an energy of 2.4 mJ, and is used to generate ultrasonic waves in our samples. The pulsed laser allows

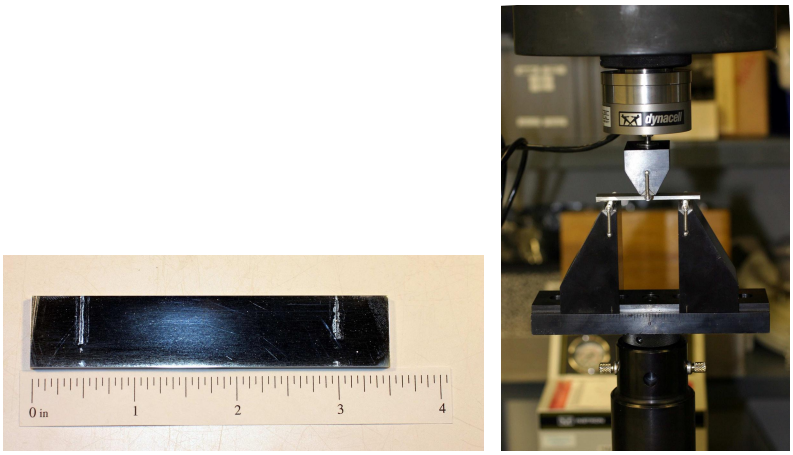

(a) Al-2024 plate

(b) Experimental setup for three-point bend fatiguing

Figure 1. Three-point bend fatiguing of the aluminum plates.

for non-contact ultrasonic acquisition as well as the ability to control the ultrasonic amplitude without material ablation. As a result, the bulk of the material undergoes no physical changes. The ultrasonic wave surface displacement is measured in transmission mode using a path-stabilized, Michelson-type interferometer with a flat frequency response from 1-60 MHz. This instrument is very sensitive to room vibrations. To control this, a vibration isolated work station is used to maximize the sensitivity of the interferometer to surface displacement. This isolation also fulfills our need to record consistent waveforms.

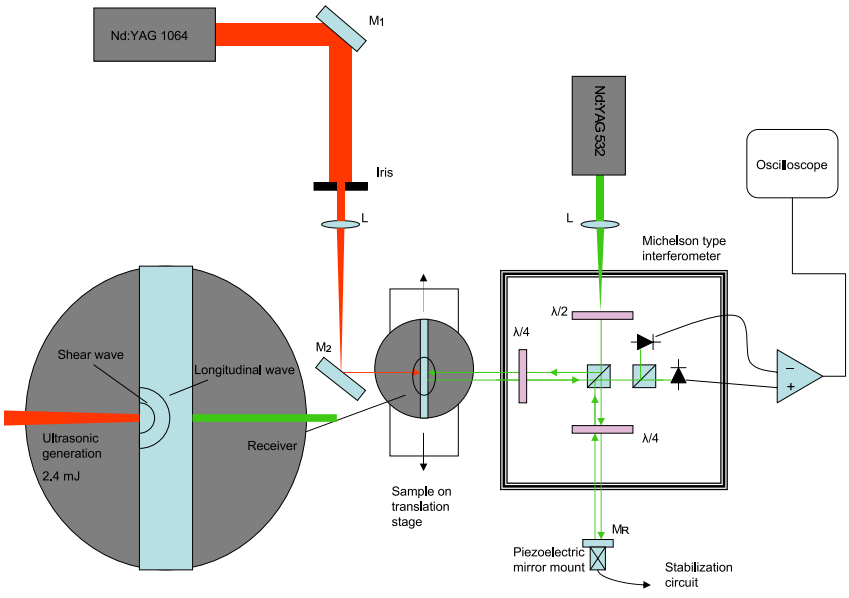

Figure 2. Schematic showing the experimental setup for ultrasonic based detection of fatigue damage in aluminum plates.

To collect ultrasonic information localized to regions that are suspected to contain fatigue damage in the sample, the source and receiver lasers are focused (0.1 mm diameters) in an epicentral configuration (source directly opposite to receiver) allowing for precise determination of ultrasonic properties. The sample is manually

translated in 0.5 mm steps while the source and receiver generate and gather ultrasonic information as a function of position. After irradiating the sample, the interferometer output is recorded by a digital oscilloscope. The waveform is digitized at a sampling rate of 10 GHz providing significant oversampling and ensuring complete characterization of noise characteristics. For a reasonable signal-to-noise ratio, 30 waveforms are averaged to eliminate the noise generated by the pulsed laser.

A typical waveform is shown in Figure 3(a), with t_L and t_S indicating the arrival times for the longitudinal and shear waves, respectively. The step displacements of the longitudinal and shear waves are A_{LS} and A_{SS}, and the noise at time zero is light from the generation laser entering the interferometer photodetectors - this helps establish time zero. The epicentral ultrasonic displacement essentially follows previously known results and established models for laser generated ultrasound in metals.[10]

Data was collected for three different structural conditions (classes): unfatigued sample, sample fatigued to 10,000 cycles, and sample fatigued to 20,000 cycles. About 15 signals were available for each class.

3.2 Preprocessing

The measured signals were first lowpass filtered and down-sampled. This was followed by time-alignment, mean removal, and normalization. The preprocessing steps are illustrated in Figures 3(b)-3(e). The plots show the signals from the three classes. Figure 3(f) shows the time-domain correlations between the signals. While the block diagonal structure of the correlation plot is quite evident (signals from the same class correlate better than those from different classes), we see that the correlation values themselves are not very different. A classifier based simply on time-domain correlations is therefore not expected to be very robust to noise.

3.3 MMPD Classifier and Choice of Parameters

Figure 4 shows plots of the signals both in the time-domain and time-frequency plane. The latter is useful for analyzing the time-varying spectral content of the signals. The time-frequency representation (TFR) used here for this purpose is the Short-Time Fourier Transform (STFT).[11] We employ the STFT with a Gaussian window (known for its good time-frequency localization properties), so that good resolution is retained both in time and frequency. From the TFR plots we see that the shear waves are more attenuated in the fatigued samples as compared to the unfatigued case, especially at the higher frequencies. The MMPD time-frequency based technique performs damage classification by exploiting these differences between the signals for the various structural conditions.

Half of the available data was used for constructing the MMPD dictionary (training data), and the remaining half was used for testing the classifier performance. Only one MMPD iteration was performed to decompose the test signals, because this was found to be sufficient to reduce the residue energy to less than 20%.

Upon testing, our MMPD classifier resulted in correct classification for all the tested data and this is quite promising. However, the size of the data set was too small to make any significant claims.

4. CONCLUSION

In this paper, we have presented a structural damage classification technique based on ultrasonic sensing and time-frequency analysis. Ultrasonic measurements taken across a fatigue damaged region in Al-6061 and Al-2024 plates show that the material stiffness is largely unaffected by damage, but that attenuation (here related to ultrasonic amplitudes) is related to damage. This can be seen by comparing longitudinal and shear amplitudes of waveforms from various regions.

Data collected by ultrasonic sensors is decomposed into a time-frequency basis using the MMPD algorithm. The resulting compact representation is then utilized to classify structural damage based on the strengths of projections onto various damage classes. Application to the detection of fatigue damage in Al-6061 and Al-2024 plates shows that the performance of the damage classifier is quite good. Note that, while we observe near perfect correct classification rates, the size of our present data set is quite limited (only about 15 signals for each class). Both experimental and modeling effort is underway to obtain a sample set that is more statistically representative.

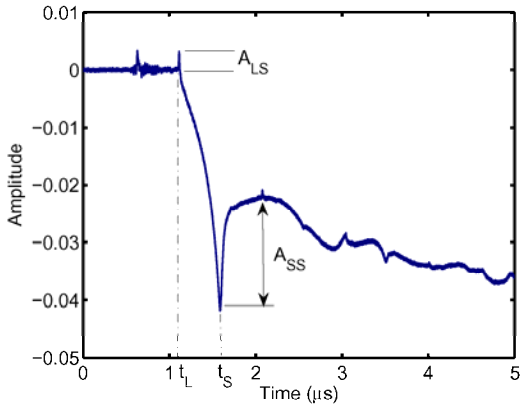

(a) An example signal for the unfatigued case

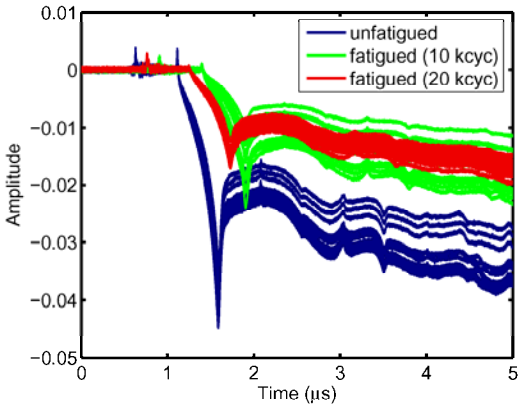

(b) Raw signals

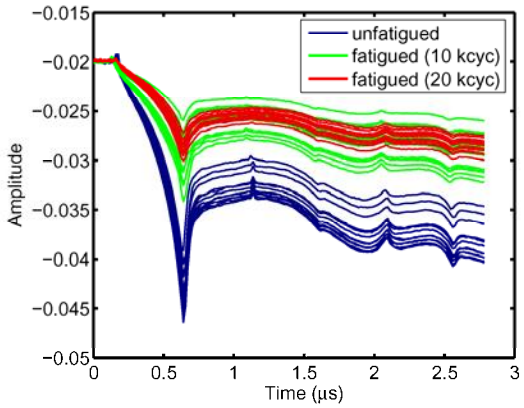

(c) Signals after low-pass filtering and time-alignment

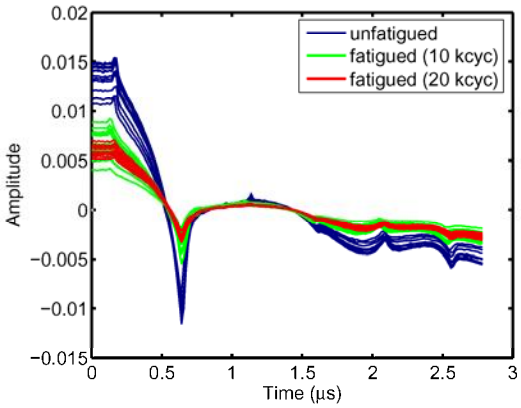

(d) Signals after mean removal

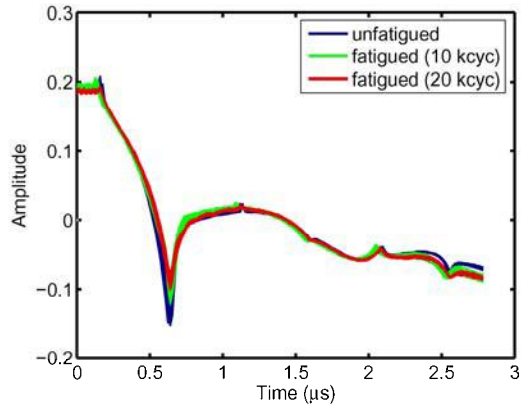

(e) Signals after normalization

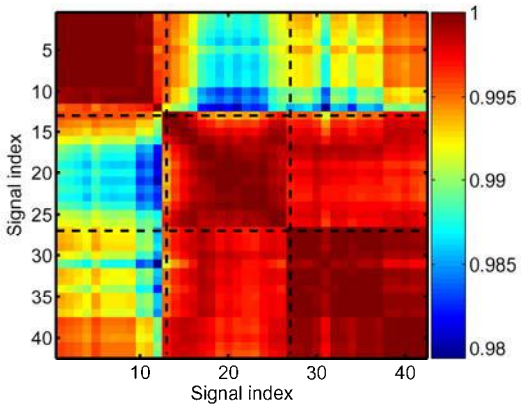

(f) Signal correlations

Figure 3. Data and preprocessing.

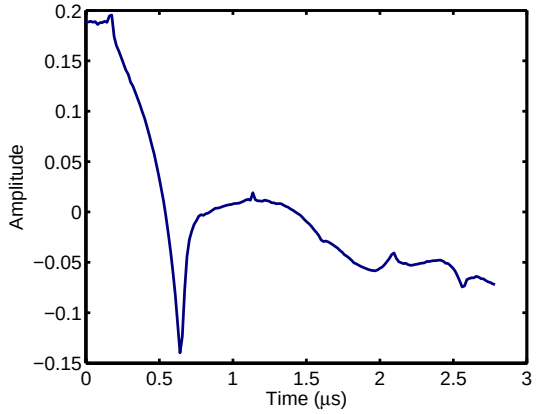

(a) Example signal (unfatigued)

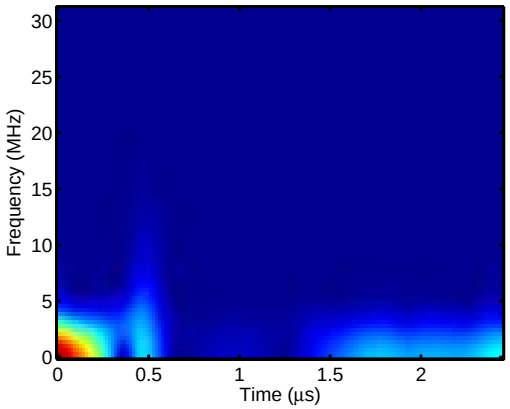

(b) Example signal STFT (unfatigued)

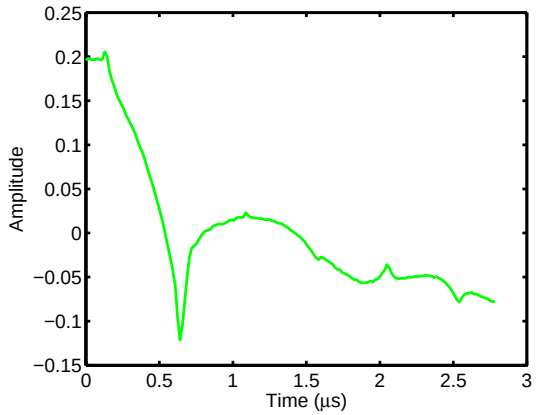

(c) Example signal (10 kcycles fatigued)

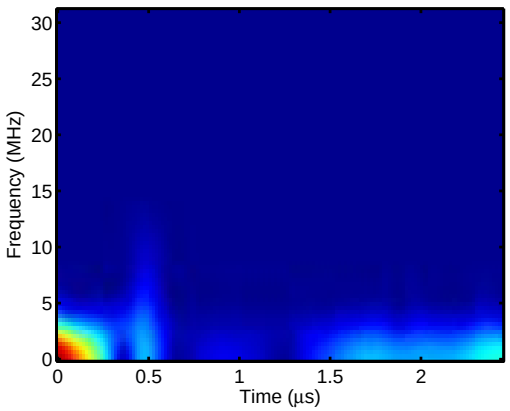

(d) Example signal STFT (10 kcycles fatigued)

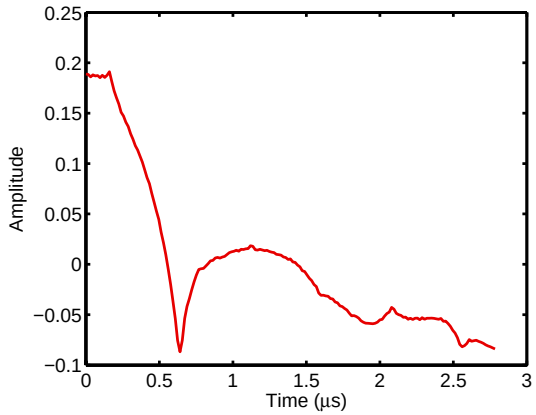

(e) Example signal (20 kcycles fatigued)

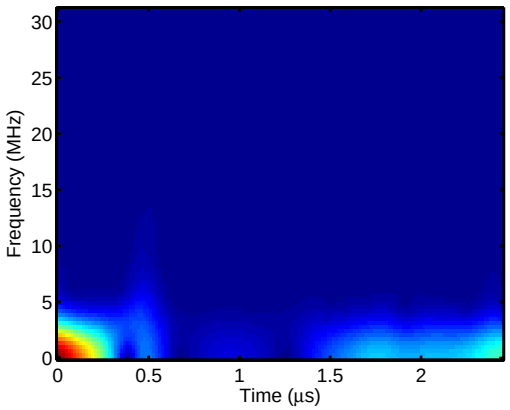

(f) Example signal STFT (20 kcycles fatigued)

Figure 4. Example plots showing representative (preprocessed) signals from the three classes and the corresponding Short-Time Fourier Transforms (STFTs).

In conclusion, we have demonstrated that results from non-destructive evaluation (NDE) can be used in conjunction with novel classification techniques to detect damage at very small (micro) length scales for which off-the-shelf sensors and vibration/impedance/conventional wave based techniques cannot be used.

ACKNOWLEDGMENTS

This research was supported by the MURI Program, Air Force Office of Scientific Research, grant number: FA9550-06-1-0309; Technical Monitor, Dr. Victor Giurgiutiu.

REFERENCES

[1] Farrar, C. R. and Worden, K., "An introduction to structural health monitoring," *Philosophical Transactions of the Royal Society A* **365**, 303–315 (2007).

[2] Farrar, C. R. and Lieven, N. A. J., "Damage prognosis: the future of structural health monitoring," *Philosophical Transactions of the Royal Society A* **365**, 623–632 (2007).

[3] Staszewski, W. J., Boller, C., and Tomlinson, G. R., [*Health Monitoring of Aerospace Structures*], Wiley, England (2003).

[4] Blodgett, D. W. and Baldwin, K. C., "Laser-based ultrasonics: Applications at APL," *Johns Hopkins APL technical digest* **26**, 36–45 (2005).

[5] Arias, I. and Achenbach, J. D., "A model for the ultrasonic detection of surface-breaking cracks by the scanning laser source technique," *Wave Motion* **39**, 61–75 (2004).

[6] Mi, B. and Ume, I. C., "Parametric studies of laser generated ultrasonic signals in ablative regime: time and frequency domains," *Journal of Nondestructive Evaluation* **21**, 23–33 (2002).

[7] Scruby, C. B., Dewhurst, R. J., Hutchins, D. A., and Palmer, S. B., "Quantitative studies of thermally generated elastic waves in laser-irradiated metals," *Journal of Applied Physics* **51**, 6210–6216 (1980).

[8] Cielo, P., Nadeau, F., and Lamontagne, M., "Laser generation of convergent acoustic waves for materials inspection," *Ultrasonics* **23**, 55–62 (1985).

[9] Ogi, H., Hirao, M., and Minoura, K., "Noncontact measurement of ultrasonic attenuation during rotating fatigue test of steel," *Journal of Applied Physics* **81**, 3677–3684 (1997).

[10] Rose, L. R. F., "Point-source representation for laser-generated ultrasound," *Journal of the Acoustical Society of America* **75**, 723–732 (1984).

[11] Papandreou-Suppappola, A., ed., [*Applications in Time-Frequency Signal Processing*], CRC Press, Florida (2002).

[12] Mallat, S. G. and Zhang, Z., "Matching pursuits with time-frequency dictionaries," *IEEE Transactions on Signal Processing* **41**, 3397–3415 (1993).

[13] Papandreou-Suppappola, A. and Suppappola, S. B., "Adaptive time-frequency representations for multiple structures," in [*Proc. 10th IEEE Workshop on Statistical Signal and Array Processing*], **3** (2000).

[14] Ebenezer, S. P., Papandreou-Suppappola, A., and Suppappola, S. B., "Matching pursuit classification for time-varying acoustic emissions," in [*35th Asilomar Conference on Signals, Systems and Computers*], 715–719 (2001).

[15] Ebenezer, S. P., Papandreou-Suppappola, A., and Suppappola, S. B., "Classification of acoustic emissions using modified matching pursuit," *EURASIP Journal on Applied Signal Processing* **3**, 347–357 (2004).

[16] Ebenezer, S. P., *Classification of time-varying signals from an acoustic monitoring system using time-frequency techniques*, Master's thesis, Arizona State University, Tempe, AZ (December 2001).

[17] Papandreou-Suppappola, A. and Suppappola, S. B., "Analysis and classification of time-varying signals with multiple time-frequency structures," *IEEE Signal Processing Letters* **9**, 92–95 (2002).

[18] Das, S., Papandreou-Suppappola, A., Zhou, X., and Chattopadhyay, A., "On the use of the matching pursuit decomposition signal processing technique for structural health monitoring," *Proc. of SPIE* **5764**, 583–594 (2005).

[19] Kovvali, N., Das, S., Chakraborty, D., Cochran, D., Papandreou-Suppapola, A., and Chattopadhyay, A., "Time-frequency based classification of structural damage," *48th AIAA/ASME/ASCE/AHS/ASC Structures, Structural Dynamics, and Materials Conference* , AIAA 2007–2055 (Honolulu, Hawaii, 23 - 26 April 2007).

[20] Zhou, W., Kovvali, N., Papandreou-Suppappola, A., Cochran, D., and Chattopadhyay, A., "Hidden Markov model based classification of structural damage," *Proc. of SPIE* **6523**, 652311 (2007).